Semileptonic $B^- \to \pi^+\pi^-\ell^-\bar{\nu}_\ell$ decay with $\pi\pi$ invariant mass spectrum

Shang-Yuu Tsai[1,*] and Yu-Kuo Hsiao[1,†]

[1]*School of Physics and Information Engineering, Shanxi Normal University, Linfen 041004, China*

(Dated: November 16, 2021)

Abstract

BELLE has recently reported the measurement of the branching fraction of the semileptonic $B^- \to \pi^+\pi^-\ell^-\bar{\nu}_\ell$ decay, where ℓ represents an electron or a muon. With the new information on the $\pi\pi$ invariant mass spectrum, we extract $|V_{ub}| = (3.31 \pm 0.61) \times 10^{-3}$ in agreement with those from the other exclusive B decays. In particular, we determine the non-resonant $B \to \pi\pi$ transition form factors, and predict the non-resonant branching fraction $\mathcal{B}(B^- \to \pi^+\pi^-\ell^-\bar{\nu}_\ell) = (3.5 \pm 1.4^{+4.3}_{-2.4}) \times 10^{-5}$, which is accessible to the BELLEII and LHCb experiments.

* shangyuu@gmail.com

† yukuohsiao@gmail.com

I. INTRODUCTION

For the Cabibbo-Kobayashi-Maskawa (CKM) matrix element $|V_{ub}|$, there have been the long-standing inconsistent determinations from the inclusive and exclusive b-hadron decays [1, 2], which might indicate the existence of new physics [3–11]. For a careful examination, the exclusive $B^- \to \pi^+\pi^-\ell^-\bar{\nu}_\ell$ decay can provide another path to determining $|V_{ub}|$, where ℓ represents an electron or a muon. Nonetheless, although $B^- \to \pi^+\pi^-\ell^-\bar{\nu}_\ell$ has been observed many times [13–16], it is essentially $B^- \to \rho^0\ell^-\bar{\nu}_\ell$ along with $\rho^0 \to \pi^+\pi^-$, instead of a genuine four-body decay.

Recently, BELLE has newly reported the measurement of the branching fractions of $B^- \to \pi^+\pi^-\ell^-\bar{\nu}_\ell$ with the full $\pi\pi$ invariant mass ($M_{\pi\pi}$) spectrum [17]. In addition to the resonant processes of $B^- \to R\ell^-\bar{\nu}_\ell, R \to \pi^+\pi^-$ with $R = \rho^0$ and $f_2 \equiv f_2(1270)$, the non-resonant contribution is also found. Explicitly, we present the branching fractions as [1, 17, 18]

$$
\begin{aligned}
&\mathcal{B}_{\rm T}(B^- \to \pi^+\pi^-\ell^-\bar{\nu}_\ell) = (22.7^{+1.9}_{-1.6} \pm 3.4) \times 10^{-5}\,,\\
&\mathcal{B}_{\rho}(B^- \to \rho^0\ell^-\bar{\nu}_\ell, \rho^0 \to \pi^+\pi^-) = (15.8 \pm 1.1) \times 10^{-5}\,,\\
&\mathcal{B}_{f_2}(B^- \to f_2\ell^-\bar{\nu}_\ell, f_2 \to \pi^+\pi^-) = (1.8 \pm 0.9^{+0.2}_{-0.1}) \times 10^{-5}\,,\\
&\mathcal{B}_{\rm N}(B^- \to \pi^+\pi^-\ell^-\bar{\nu}_\ell) = (5.1 \pm 4.3) \times 10^{-5}\,,
\end{aligned}
\tag{1}
$$

where $\mathcal{B}_{\rm T,N}$ denote the total and non-resonant branching fractions, respectively, while $\mathcal{B}_\rho \simeq \mathcal{B}(B^- \to \rho^0\ell^-\bar{\nu}_\ell) \times \mathcal{B}(\rho^0 \to \pi^+\pi^-)$ is from PDG [1]. By excluding $\mathcal{B}_{\rho,f_2}$ from $\mathcal{B}_{\rm T}$, we estimate $\mathcal{B}_{\rm N}$ in Eq. (1).

As depicted in Fig. 1, $B^- \to \pi^+\pi^-\ell^-\bar{\nu}_\ell$ proceeds through the resonant and non-resonant $B \to \pi\pi$ transitions, respectively, with the lepton-pair produced from the emitted W-boson. One has been enabled to parameterize the resonant $B \to \rho(f_2), \rho(f_2) \to \pi\pi$ transition [19]. Despite the theoretical attempts [5, 12, 20–29], the non-resonant $B \to \pi\pi$ transition is still poorly understood. With the full $\pi\pi$ invariant mass spectrum provided for the first time, the information on the non-resonant $B \to \pi\pi$ transition form factors ($F_{\pi\pi}$) becomes available. Hence, we propose to newly extract $|V_{ub}|$ and $F_{\pi\pi}$, by which we will be able to study $\mathcal{B}_{\rm N}$. We will also study the angular distribution and its asymmetry to be compared to the future measurements.

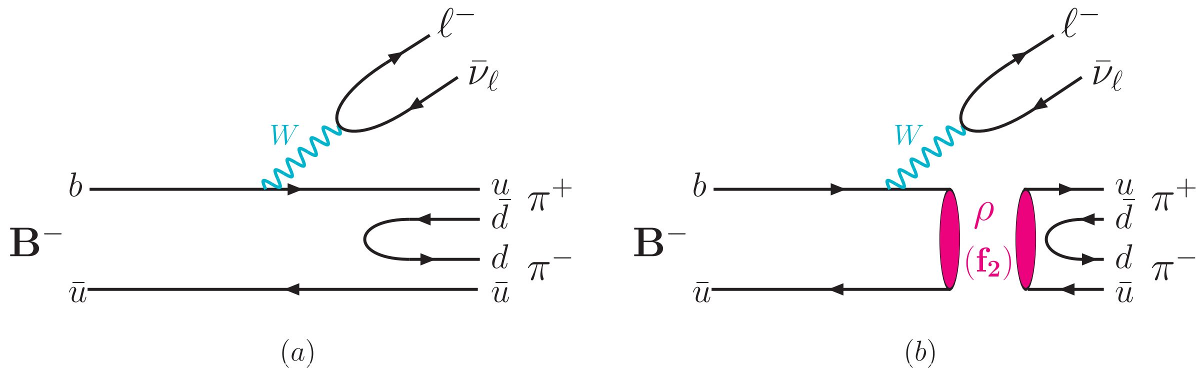

FIG. 1. $B^- \to \pi^+\pi^-\ell^-\bar{\nu}_\ell$ with (a) non-resonant and (b) resonant contributions.

II. THEORETICAL FRAMEWORK

The semileptonic $B^- \to \pi^+\pi^-\ell^-\bar{\nu}_\ell$ decay is observed with the full $M_{\pi\pi}$ spectrum, which indicates the existence of the non-resonant contribution [17]. Moreover, the simulation is performed to seek the resonances that contribute to $B^- \to \pi^+\pi^-\ell^-\bar{\nu}_\ell$. It turns out that only a dominant peak and a small bump are observed, which correspond to $B^- \to \rho^0\ell\bar{\nu}$, $f_2\ell\bar{\nu}$, respectively, with $\rho^0, f_2 \to \pi^+\pi^-$. Therefore, the total amplitude of $B^- \to \pi^+\pi^-\ell^-\bar{\nu}_\ell$ can be written as

$$\begin{aligned}
\mathcal{M}_{\rm T} &= \mathcal{M}_{\rm N}(B^- \to \pi^+\pi^-\ell\bar{\nu}_\ell) + \mathcal{M}_\rho(B^- \to \rho^0\ell^-\bar{\nu}_\ell, \rho^0 \to \pi^+\pi^-) \\
&\quad + \mathcal{M}_{f_2}(B^- \to f_2\ell^-\bar{\nu}_\ell, f_2 \to \pi^+\pi^-)\,, \\
\mathcal{M}_{\rm N(R)} &= \frac{G_F V_{ub}}{\sqrt{2}} \langle \pi^+\pi^- | \bar{u}\gamma_\mu(1-\gamma_5)b|B^-\rangle_{\rm N(R)}\, \bar{u}_\ell \gamma^\mu(1-\gamma_5)v_\nu\,,
\end{aligned} \tag{2}$$

with $R = (\rho, f_2)$. The matrix elements of the (non-)resonant B meson to $\pi\pi$ transitions can be parameterized as [12, 30]

$$\begin{aligned}
&\langle \pi^+(p_a)\pi^-(p_b)|\bar{u}\gamma_\mu(1-\gamma_5)b|B^-\rangle_N \\
&= h\epsilon_{\mu\nu\alpha\beta}p_B^\nu p^\alpha (p_b-p_a)^\beta + irq_\mu + iw_+p_\mu + iw_-(p_b-p_a)\,, \\
&\langle \pi^+(p_a)\pi^-(p_b)|\bar{u}\gamma_\mu(1-\gamma_5)b|B^-\rangle_{\rho(f_2)} \\
&= \langle \pi^+\pi^-|\rho(f_2)\rangle \frac{i}{(t-m^2_{\rho(f_2)}) + im_{\rho(f_2)}\Gamma_{\rho(f_2)}} \langle \rho(f_2)|\bar{u}\gamma_\mu(1-\gamma_5)b|B^-\rangle\,,
\end{aligned} \tag{3}$$

with $p = p_b + p_a$, $q = p_B - p = p_\ell + p_\nu$, $(s,t) \equiv (q^2, p^2)$, and the form factors $F_{\pi\pi} = (h, r, w_\pm)$. The matrix elements of $B \to \rho(f_2)$ transition are written as [33–35]

$$
\begin{aligned}
\langle \rho(f_2)|\bar{u}\gamma_\mu b|B\rangle &= \epsilon_{\mu\nu\alpha\beta}\epsilon^{(\prime)\nu}p_B^\alpha p_{\rho(f_2)}^\beta \frac{2V_1^{(\prime)}}{m_B+m_{\rho(f_2)}}\,,\\
\langle \rho(f_2)|\bar{u}\gamma_\mu\gamma_5 b|B\rangle &= i\Big[\epsilon_\mu^{(\prime)}-\frac{\epsilon^{(\prime)}\cdot p_B}{s}q_\mu\Big](m_B+m_{\rho(f_2)})A_1^{(\prime)}+i\frac{\epsilon^{(\prime)}\cdot p_B}{s}q_\mu(2m_{\rho(f_2)})A_0^{(\prime)}\\
&\quad -i\Big[(p_B+p_{\rho(f_2)})_\mu-\frac{m_B^2-m_{\rho(f_2)}^2}{s}q_\mu\Big](\epsilon^{(\prime)}\cdot p_B)\frac{A_2^{(\prime)}}{m_B+m_{\rho(f_2)}}\,,
\end{aligned}
\tag{4}
$$

with $\epsilon'^{\mu}\equiv\epsilon^{\mu\nu}p_{B\nu}/m_B$ and the form factors $F_{\rho(f_2)}=(V_1^{(\prime)},A_{0,1,2}^{(\prime)})$, where ϵ^ν and $\epsilon^{\mu\nu}$ are the polarization vector and tensor, respectively. To describe the $\rho^0, f_2\to\pi^+\pi^-$ decays, $\langle\pi\pi|\rho,f_2\rangle$ in Eq. (2) are given by [9, 19, 36]

$$
\begin{aligned}
\langle\pi\pi|\rho\rangle &= g_1\epsilon\cdot(p_b-p_a)\,,\\
\langle\pi\pi|f_2\rangle &= g_2\epsilon^{\mu\nu}p_{a\mu}p_{b\nu}\,,
\end{aligned}
\tag{5}
$$

where $g_{1,2}$ are strong coupling constants. To sum over the vector and tensor spins for ρ and f_2, respectively, as the intermediate states in the resonant $B\to\pi\pi$ transitions, we use the following identities [33–35],

$$
\begin{aligned}
\Sigma\epsilon_\mu\epsilon^*_{\mu'} &= M_{\mu\mu'}\,,\\
\Sigma\epsilon_{\mu\nu}\epsilon^*_{\mu'\nu'} &= \frac{1}{2}M_{\mu\mu'}M_{\nu\nu'}+\frac{1}{2}M_{\mu\nu'}M_{\nu\mu'}-\frac{1}{3}M_{\mu\nu}M_{\mu'\nu'}\,,
\end{aligned}
\tag{6}
$$

with $M_{\mu\mu'}=-g_{\mu\mu'}+p_\mu p_{\mu'}/p^2$. The form factors in Eqs. (3, 4) are momentum-dependent, modelled in the single-pole or double-pole forms [33–35]:

$$
\begin{aligned}
F_\rho(s) &= \frac{F_\rho(0)}{1-s/m_V^2}\,,\\
F_{f_2}(s) &= \frac{F_{f_2}(0)}{(1-s/m_B^2)^2}\,,\\
F_{\pi\pi}(t) &= \frac{F_{\pi\pi}(0)}{1-a\,(t/m_B^2)+b\,(t/m_B^2)^2}\,,
\end{aligned}
\tag{7}
$$

where $F_{\rho,f_2}(s)$ have been studied in QCD models, whereas $(a,b,F_{\pi\pi}(0))$ need to be extracted in the global fit.

For the four-body decay channel $B^-(p_B)\to\pi^+(p_a)\pi^-(p_b)\ell^-(p_\ell)\bar\nu_\ell(p_\nu)$, one has to integrate over the kinematic variables $(s,t,\theta_M,\theta_L,\phi)$ in the phase space. See Fig. 2, $\theta_{M(L)}$ is the angle between π^+ and π^- (ℓ^- and $\bar\nu_\ell$) moving directions in the $\pi^+\pi^-$ ($\ell^-\bar\nu_\ell$) rest frame. In addition, the angle ϕ is between the $\pi^+\pi^-$ and $\ell^-\bar\nu_\ell$ planes, defined by $\vec{p}_{a,b}$ and $\vec{p}_{\ell,\bar\nu_\ell}$,

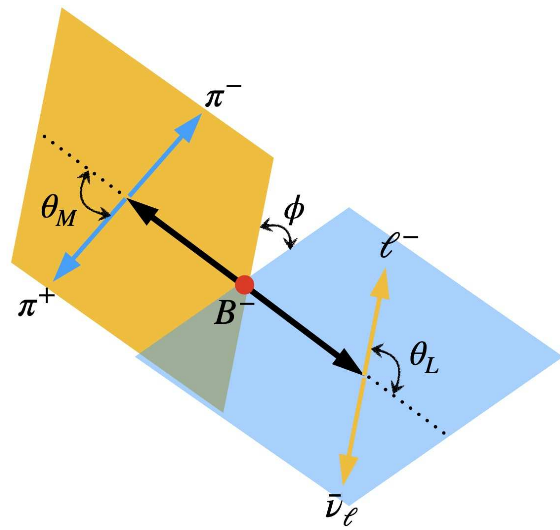

FIG. 2. The angular variables $(\theta_M, \theta_L, \phi)$ in the four-body $B^- \to \pi^+\pi^-\ell^-\bar{\nu}_\ell$ decay.

respectively, in the B-meson rest frame. Then, the partial decay width reads [37, 38]

$$d\Gamma = \frac{|\mathcal{M}|^2}{4(4\pi)^6 m_B^3} X \alpha_M \alpha_L \, ds \, dt \, d\cos\theta_M \, d\cos\theta_L \, d\phi \,, \tag{8}$$

where X, α_M and α_L are defined by

$$\begin{aligned} X &= \left[\frac{1}{4}(m_B^2 - s - t)^2 - st\right]^{1/2} , \\ \alpha_M &= \frac{1}{t}\lambda^{1/2}(t, m_\pi^2, m_\pi^2) \,, \\ \alpha_L &= \frac{1}{s}\lambda^{1/2}(s, m_\ell^2, m_{\bar{\nu}}^2) \,, \end{aligned} \tag{9}$$

with $\lambda(a,b,c) = a^2 + b^2 + c^2 - 2ab - 2bc - 2ca$. The allowed ranges for (s,t) and the angular variables $(\theta_M, \theta_L, \phi)$ are given by

$$\begin{aligned} (m_\ell + m_{\bar{\nu}_\ell})^2 \leq s \leq (m_B - \sqrt{t})^2 \,, \\ 4m_\pi^2 \leq t \leq (m_B - m_\ell - m_{\bar{\nu}_\ell})^2 \,, \\ 0 \leq \theta_{M,L} \leq \pi \,, \\ 0 \leq \phi \leq 2\pi \,, \end{aligned} \tag{10}$$

with $m_\ell + m_{\bar{\nu}_\ell} \simeq 0$. From Eq. (8), we define the angular distribution asymmetry as

$$A_{\theta_M} \equiv \frac{\int_0^{+1} \frac{d\Gamma}{d\cos\theta_M} d\cos\theta_M - \int_{-1}^{0} \frac{d\Gamma}{d\cos\theta_M} d\cos\theta_M}{\int_0^{+1} \frac{d\Gamma}{d\cos\theta_M} d\cos\theta_M + \int_{-1}^{0} \frac{d\Gamma}{d\cos\theta_M} d\cos\theta_M} \,, \tag{11}$$

where $d\Gamma/d\cos\theta_M$ is the angular distribution.

TABLE I. The B to (ρ, f_2) transition form factors with $M_V = 7.0$ GeV in Eq. (7) [32, 34]. Here, we present $\sqrt{2}F_{\rho^0} = F_\rho$ for the B to ρ^0 transition.

	$V_1^{(\prime)}$	$A_1^{(\prime)}$	$A_2^{(\prime)}$
$\sqrt{2}F_{\rho^0}(0)$	$0.35^{+0.06}_{-0.05}$	$0.27^{+0.05}_{-0.04}$	$0.26^{+0.05}_{-0.03}$
$F_{f_2}(0)$	(0.18 ± 0.02)	(0.13 ± 0.02)	(0.12 ± 0.02)

III. NUMERICAL ANALYSIS

In the numerical analysis, we perform the minimum χ^2-fit, in order to extract $|V_{ub}|$, $F_{\pi\pi}$ and $\delta_{1,2}$ as the free parameters, where $\delta_{1(2)}$ is the relative phase for $\mathcal{A}_{\rho(f_2)}$. The equation of the χ^2-fit is given by

$$\chi^2 = \left(\frac{\mathcal{B}_{\rho\, th} - \mathcal{B}_{\rho\, ex}}{\sigma_{\rho\, ex}}\right)^2 + \left(\frac{\mathcal{B}_{f_2\, th} - \mathcal{B}_{f_2\, ex}}{\sigma_{f_2\, ex}}\right)^2 + \sum_i \left(\frac{\frac{d\mathcal{B}^i_{th}}{dM_{\pi\pi}} - \frac{d\mathcal{B}^i_{ex}}{dM_{\pi\pi}}}{\sigma^i_{ex}}\right)^2 + \sum_j \left(\frac{F^j_{\rho(f_2)} - F^j_{th\,\rho(f_2)}}{\delta F^j_{th\,\rho(f_2)}}\right)^2 , \tag{12}$$

where $d\mathcal{B}/dM_{\pi\pi}$ denotes the partial branching ratio, and σ_{ex} (δF_{th}) the uncertainty from the observation (form factor). $\mathcal{B}_{\rho(f_2)\,th}$ and $d\mathcal{B}_{th}/dM_{\pi\pi}$ are the theoretical inputs from the amplitudes in Eq. (2), and the experimental inputs are given in Eq. (1) and Fig. 3. We take F_ρ and F_{f_2} in Table I as the initial values in Eq. (12), together with $|g_1| = 5.98$ and $|g_2| = 18.56$ GeV^{-1} [36, 39].

Subsequently, we extract that

$$\begin{aligned}
&|V_{ub}| = (3.31 \pm 0.61) \times 10^{-3} ,\\
&a = (0.96 \pm 0.93) \times m_B^2,\ b = (1.84 \pm 0.87) \times m_B^4,\\
&h(0) = 1.90 \pm 0.43 ,\ w_+(0) = 6.16 \pm 3.41 ,\ w_-(0) = 3.67 \pm 1.79 ,\\
&(\delta_1, \delta_2) = (-111.6 \pm 29.3, 0.0 \pm 1.4)^\circ\\
&\chi^2/n.d.f = 1.1 ,
\end{aligned} \tag{13}$$

with $n.d.f = 7$ the number of degrees of freedom. The form factors $V_1^{(\prime)}$ and $A_{1,2}^{(\prime)}$ are fitted to slightly deviate from their initial inputs in Table I, given by

$$\begin{aligned}
&(V_1(0), A_1(0), A_2(0)) = (0.35 \pm 0.06, 0.29 \pm 0.04, 0.28 \pm 0.04) ,\\
&(V_1'(0), A_1'(0), A_2'(0)) = (0.18 \pm 0.02, 0.11 \pm 0.02, 0.14 \pm 0.02) .
\end{aligned} \tag{14}$$

Nonetheless, r and $A_0^{(\prime)}$ in Eqs. (3, 4) are not involved in the global fit, since they have been vanishing with $q_\mu \bar{u}_\ell \gamma^\mu (1-\gamma_5) v_\nu = 0$ in the amplitudes, where the lepton pair is nearly massless.

Using the fit results in Eqs. (13,14), we obtain

$$\begin{aligned}
&\mathcal{B}_{\rm T}(B^- \to \pi^+\pi^-\ell^-\bar{\nu}_\ell) = (19.6 \pm 7.9^{+7.5+0.7}_{-5.4-0.1}) \times 10^{-5}\,, \\
&\mathcal{B}_\rho(B^- \to \rho^0\ell^-\bar{\nu}_\ell, \rho^0 \to \pi^+\pi^-) = (15.8 \pm 6.4^{+7.1}_{-5.7}) \times 10^{-5}\,, \\
&\mathcal{B}_{f_2}(B^- \to f_2\ell^-\bar{\nu}_\ell, f_2 \to \pi^+\pi^-) = (2.6 \pm 1.1^{+1.2}_{-0.9}) \times 10^{-5}\,, \\
&\mathcal{B}_{\rm N}(B^- \to \pi^+\pi^-\ell^-\bar{\nu}_\ell) = (3.5 \pm 1.4^{+4.3}_{-2.4}) \times 10^{-5}\,,
\end{aligned} \tag{15}$$

where the first errors are from $|V_{ub}|$, the second ones from the form factors, and the third error for $\mathcal{B}_T$ from the relative phase δ_1. Moreover, we draw the partial branching fractions as the functions of $M_{\pi\pi}$ and $\cos\theta_M$ in Fig. 3 and Fig. 4, respectively. We also calculate the angular distribution asymmetries, given by

$$\begin{aligned}
&A_{\theta_M,{\rm T}}(B^- \to \pi^+\pi^-\ell^-\bar{\nu}_\ell) = (1.3 \pm 8.9^{+0.8}_{-2.5})\%\,, \\
&A_{\theta_M,\rho}(B^- \to \rho^0\ell^-\bar{\nu}_\ell, \rho^0 \to \pi^+\pi^-) = (0.20 \pm 0.04)\%\,, \\
&A_{\theta_M,f_2}(B^- \to f_2\ell^-\bar{\nu}_\ell, f_2 \to \pi^+\pi^-) = (0.31 \pm 0.08)\%\,, \\
&A_{\theta_M,{\rm N}}(B^- \to \pi^+\pi^-\ell^-\bar{\nu}_\ell) = (-43.0 \pm 22.3)\%\,,
\end{aligned} \tag{16}$$

where the first errors come from the uncertainties of the form factors, and the second error for $A_{\theta_M,{\rm T}}$ is from the relative phase δ_1.

IV. DISCUSSIONS AND CONCLUSIONS

We study $B^- \to \pi^+\pi^-\ell\bar{\nu}$, in order to explain the $\pi\pi$ invariant mass spectrum observed by BELLE [17]. In Fig. 3, the curves for $B^- \to (\rho^0, f_2)\ell\bar{\nu}, (\rho^0, f_2) \to \pi^+\pi^-$ are shown to barely fit the first three data points in the spectrum. Nonetheless, the non-resonant $B^- \to \pi^+\pi^-\ell\bar{\nu}$ raises the contribution as the dot-dashed curve describes. As a result, the solid curve that takes into account the resonant and non-resonant contributions is able to explain the data, with $\chi^2/d.o.f = 1.1$ that presents a reasonable fit. The relative phase $\delta_1 = -111.6^\circ$ causes a destructive interference between the non-resonant $B^- \to \pi^+\pi^-\ell\bar{\nu}$ and $B^- \to \rho^0\ell\bar{\nu}, \rho^0 \to \pi^+\pi^-$. As a demonstration, we turn off δ_1 and obtain $\mathcal{B}_T = 22.2 \times 10^{-5}$. By contrast, δ_2 is fitted to be zero, in accordance with the fact that the non-resonant

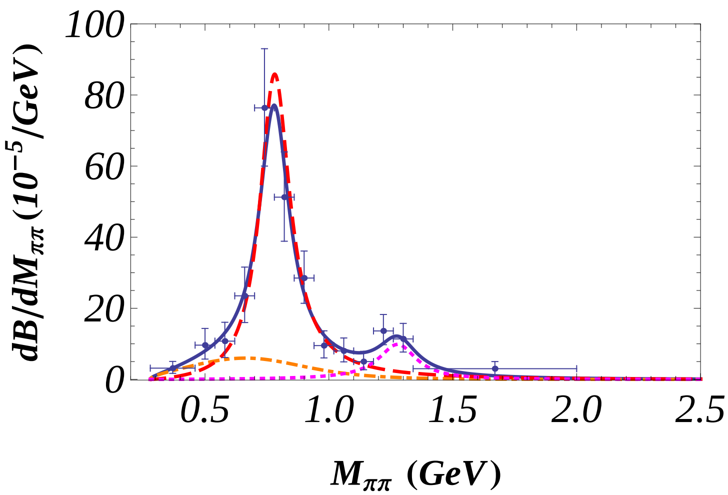

FIG. 3. The $\pi\pi$ invariant mass spectrum, where the solid curve that takes into account the all contributions explains the data points from BELLE [17]. On the other hand, the dashed (dotted) and dot-dashed curves depict the contributions from $B^- \to \rho(f_2)\ell\bar{\nu}, \rho(f_2) \to \pi^+\pi^-$, and non-resonant $B^- \to \pi^+\pi^-\ell^-\bar{\nu}_\ell$, respectively.

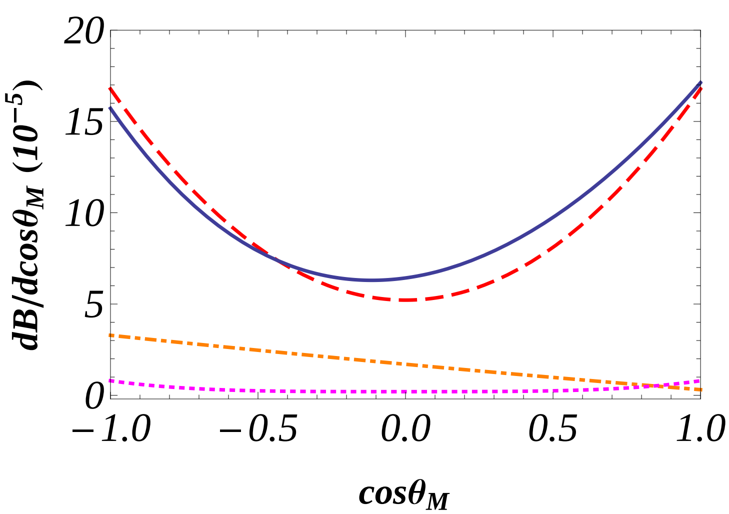

FIG. 4. Angular distributions of $B^- \to \pi^+\pi^-\ell^-\bar{\nu}_\ell$, where the solid, dashed, dotted and dot-dashed curves represent the same contributions as those in Fig. 3.

contribution is tiny in the range of $M_{\pi\pi} > 1$ GeV, barely having the interference with $B^- \to f_2\ell\bar{\nu}, f_2 \to \pi^+\pi^-$.

It turns out that $\mathcal{B}_{\rm N} = (3.5 \pm 1.4^{+4.3}_{-2.4}) \times 10^{-5}$ is given for the first time. Also importantly, we determine $|V_{ub}| = (3.31 \pm 0.61) \times 10^{-3}$ from the first genuine four-body semileptonic $B \to$

$\pi\pi\ell\bar\nu$ decay, instead of $B^-\to\rho^0\ell\bar\nu, \rho^0\to\pi^+\pi^-$. For the angular distribution asymmetries, we obtain $A_{\theta_M,\rho(f_2)}=0$, showing the symmetric distributions as the curves in Fig. 4. By contrast, $|A_{\theta_M,\rm N}|$ is as large as 40%. This is due to the main contributions from the form factors $w_+(p_b+p_a)_\mu$ and $w_-(p_b-p_a)$. With $p_b+p_a=(2E_b,\vec 0)$ and $p_b-p_a=(0,2\vec p_b)$ in the $\pi^+(p_a)\pi^-(p_b)$ rest frame (see Fig. 2), the projection of $w_\mp(p_b\mp p_a)$ onto the four-momentum of the lepton pair system causes a $\cos\theta_M$-(in)dependent term, such that their interference leads to the large angular distribution asymmetry.

In summary, we have studied the semileptonic $B^-\to\pi^+\pi^-\ell\bar\nu$ decay. With the full $\pi\pi$ invariant mass spectrum observed by BELLE, we have determined $|V_{ub}|=(3.31\pm0.61)\times10^{-3}$ agreeing with the other exclusive determinations. Besides, we have extracted the non-resonant $B\to\pi\pi$ transition form factors, by which we have predicted the non-resonant branching fraction $\mathcal{B}_{\rm N}(B^-\to\pi^+\pi^-\ell^-\bar\nu_\ell)=(3.5\pm1.4^{+4.3}_{-2.4})\times10^{-5}$. We have also predicted the non-resonant angular distribution asymmetry $A_{\theta_M,\rm N}(B^-\to\pi^+\pi^-\ell^-\bar\nu_\ell)=(-43.0\pm22.3)\%$ to be checked by the future measurements.

ACKNOWLEDGMENTS

This work was supported by National Science Foundation of China (No. 11675030).

[1] P.A. Zyla *et al.* [Particle Data Group], PTEP **2020**, 083C01 (2020).

[2] Please see PDG for a review.

[3] A. Crivellin, Phys. Rev. D **81**, 031301 (2010).

[4] A.J. Buras, K. Gemmler and G. Isidori, Nucl. Phys. B **843**, 107 (2011).

[5] X.W. Kang, B. Kubis, C. Hanhart and U.G. Meiβner, Phys. Rev. D **89**, 053015 (2014).

[6] A. Crivellin and S. Pokorski, Phys. Rev. Lett. **114**, 011802 (2015).

[7] T. Feldmann, B. Müller and D. van Dyk, Phys. Rev. D **92**, 034013 (2015).

[8] Y.K. Hsiao and C.Q. Geng, Phys. Lett. B **755**, 418 (2016).

[9] C.S. Kim, G.L. Castro and S.L. Tostado, Phys. Rev. D **95**, 073003 (2017).

[10] Y.K. Hsiao and C.Q. Geng, Eur. Phys. J. C **77**, 714 (2017).

[11] Y.K. Hsiao and C.Q. Geng, Phys. Lett. B **782**, 728 (2018).

[12] C.L.Y. Lee, M. Lu and M.B. Wise, Phys. Rev. D **46**, 5040 (1992).

[13] B. H. Behrens *et al.* [CLEO Collaboration], Phys. Rev. D **61**, 052001 (2000).

[14] T. Hokuue *et al.* [Belle Collaboration], Phys. Lett. B **648**, 139 (2007).

[15] A. Sibidanov *et al.* [Belle Collaboration], Phys. Rev. D **88**, 032005 (2013).

[16] P. del Amo Sanchez *et al.* [BaBar Collaboration], Phys. Rev. D **83**, 032007 (2011).

[17] C. Beleño *et al.* [Belle Collaboration], arXiv:2005.07766 [hep-ex].

[18] C. Beleño, "Measurement of $B \to \pi\pi\ell\bar{\nu}$ with Full Hadronic Reconstruction at Belle," thesis, Gottingen University (2018).

[19] H.Y. Cheng and C.K. Chua, Phys. Rev. D **102**, 053006 (2020).

[20] S. Fajfer, R.J. Oakes and T.N. Pham, Phys. Rev. D **60**, 054029 (1999).

[21] C.K. Chua, W.S. Hou, S.Y. Shiau and S.Y. Tsai, Phys. Rev. D **67**, 034012 (2003).

[22] C.K. Chua, W.S. Hou, S.Y. Shiau and S.Y. Tsai, Eur. Phys. J. C **33**, S253 (2004).

[23] C. Hambrock and A. Khodjamirian, Nucl. Phys. B **905**, 373 (2016).

[24] P. Boer, T. Feldmann and D.van Dyk, JHEP **1702**, 133 (2017).

[25] S. Cheng, A. Khodjamirian and J. Virto, JHEP **1705**, 157 (2017).

[26] Y.K. Hsiao and C.Q. Geng, Phys. Lett. B **770**, 348 (2017).

[27] Y.K. Hsiao, S.Y. Tsai and E. Rodrigues, Eur. Phys. J. C **80**, 565 (2020).

[28] T. Feldmann, D.Van Dyk and K.K. Vos, JHEP **1810**, 030 (2018).

[29] S. Cheng, Phys. Rev. D **99**, 053005 (2019).

[30] A. Pais and S.B. Treiman, Phys. Rev. **168**, 1858 (1968).

[31] M. Wirbel, B. Stech and M. Bauer, Z. Phys. C **29**, 637 (1985).

[32] L. Del Debbio *et al.* [UKQCD], Phys. Lett. B **416**, 392 (1998).

[33] W. Wang, Phys. Rev. D **83**, 014008 (2011).

[34] H.Y. Cheng and K.C. Yang, Phys. Rev. D **83**, 034001 (2011).

[35] Y.B. Zuo, C.X. Yue, B. Yu, Y.H. Kou, Y. Chen and W. Ling, Eur. Phys. J. C **81**, 30 (2021).

[36] M. Suzuki, Phys. Rev. D **47**, 1043 (1993).

[37] C.Q. Geng and Y.K. Hsiao, Phys. Lett. B **704**, 495 (2011).

[38] C.Q. Geng and Y.K. Hsiao, Phys. Rev. D **85**, 094019 (2012).

[39] Y.K. Hsiao, Y. Yu and B.C. Ke, Eur. Phys. J. C **80**, 895 (2020).